Available online at www.sciencedirect.com

SCIENCE DIRECT®

International Journal of Engineering Science 42 (2004) 861–885

International Journal of Engineering Science

www.elsevier.com/locate/ijengsci

On damage theory of a cohesive medium

Shaofan Li *, Gang Wang

Department of Civil and Environmental Engineering, University of California, Berkeley, CA 94720, USA

Received 2 April 2003; accepted 3 September 2003

Available online 21 February 2004

Abstract

A micro-mechanics damage model is proposed based on homogenization of penny-shaped cohesive micro-cracks (Barenblatt–Dugdale type) in a three dimensional representative volume element. By assuming that macro-hydrostatic stress state has dominant effect on permanent crack opening, a class of pressure sensitive yielding potentials and corresponding damage evolution laws have been derived. The merits of this class of damage models are: (1) Its ability to model and predict material failure and degradation due to cohesive micro-crack growth; (2) its ability to estimate the influence of Poisson's ratio on material's damage.

One of the distinguished features of the new damage model is at macro-level the reversible part of effective constitutive relation is characterized as a nonlinear elasticity, whereas the irreversible part of effective constitutive relation is a form of pressure-sensitive plasticity, both of which are significantly different from material's behaviors at micro-level before homogenization.

Keywords: Cohesive crack model; Damage; Fracture; Micro-mechanics; Plasticity

1. Introduction

Micro-mechanics modeling of materials which contain distributed defects is an important subject in reliability analysis. It has been extensively used to predict material failure and strength degradation. The popular Gurson model [13,14,38,39] is such an example, in which material's failure mechanism at micro-level is postulated to be void growth, and at macro-level the effective constitutive relation obtained from statistical averaging is a form of pressure sensitive plasticity, which depends on a damage indicator—the volume fraction of the void in a representative volume

* Corresponding author. Tel.: +1-5106425362; fax: +1-5106438928.

E-mail address: li@ce.berkeley.edu (S. Li).

0020-7225/$ - see front matter
doi:10.1016/j.ijengsci.2003.09.011

element (RVE). The most distinguished feature of the Gurson model is that its effective constitutive relation at macro-level differs from the constitutive relation at micro-level. This feature is absent in the early micro-elasticity theory, in which on both micro-level and macro-level, constitutive equations are the same, i.e., the linear elasticity—the generalized Hooke's law prevails. The *motif* of contemporary micro-mechanics is aimed at discovering unknown but vital effective constitutive information by homogenizing simple but massive micro-mechanics objects.

Failure mechanism due to void growth is supported by many experimental observations on failures of ductile materials (e.g. [9,11,32,35,41]). On the other hand, in most brittle, quasi-brittle and even some ductile materials such as concrete, rocks, ceramics and some metals, material's failure mechanism may be attributed to nucleation and coalescence of micro-cracks as well.

Although several micro-crack based damage models have been proposed to describe elastic damage processes (e.g. [5,10,20,23,29,34] and others), few micro-crack damage models are available for inelastic damage processes. Ju and co-workers [24–26] have applied micro-mechanics techniques to model effective elastoplastic behaviors of a composite with distributed inhomogeneities. In their study, qualitatively, the macro-constitutive relation of the composite is virtually the same as the micro-constitutive relation of the matrix or that of inhomogeneity—the classical elasto-plastic (J_2) constitutive relation. The objective of the approach is only to find quantitatively homogenized constitutive relations. Although the Gurson model is an exception, it is hardly a micro-mechanics model in physical sense. A basic assumption of the Gurson model is that at micro-level of an RVE the virgin material is a perfectly plastic continuum, which manifests its phenomenological limitation.

Since Barenblatt [1,2] and Dugdale's pioneer contribution [8], cohesive crack models have been studied extensively. In applications, the assessment of overall damage effect due to cohesive defect distribution is important for studying material damage at macro-level. Nevertheless, few effective constitutive models based on cohesive crack distribution are available, if there is any.

In this paper, micro-mechanics techniques are applied to study effective constitutive behaviors of a solid with randomly distributed cohesive cracks. A new cohesive damage model is derived, which is based on homogenization of randomly distributed penny-shaped cohesive cracks (Barenblatt–Dugdale type) in an elastic RVE. The cohesive damage model mimics realistic interactions among atomistic bond forces at micro-level, hence it may capture the overall damage effects due to atomistic bond break.

Before proceeding to the analysis, it may be expedient to elaborate some basic notions and hypotheses used in this study. There are several premises made in our analysis. First, the term *damage* used in this paper has specific meaning. In general, damage means material degradation caused by defects or deformation. Damage may be defined as surface separations, permanent lattice distortion, various irreversible effects due to endochronic dissipation etc. In the context of this paper, the term damage is strictly referred to the material degradation due to a specific defect—permanent crack opening, or volume fraction of permanent micro-crack opening, which may be viewed as a second phase in a composite material. This definition of damage has been extensively used in engineering literature. The definition of damage used in the Gurson model belongs to this category as well, e.g. void growth. Second, in this study we define a material's cohesive strength under hydrostatic stress state as the onset value for crack opening and surface separation. It can be related to material's yield stress by the micro-yielding condition at a crack tip.

To distinguish the damage caused by deviatoric stress, such as dislocation, disclination, and surface sliding, with the damage caused by hydrostatic stress, such as permanent crack opening, may simplify constitutive modeling. Of course, in reality, material damage may be susceptible to both hydrostatic and deviatoric stress states and it is sensitive to the combination of hydrostatic and deviatoric stress states. However, it is a reasonable approximation to assume that the damage due to permanent crack opening is only related to hydrostatic stress state, which renders the tractable homogenization solution.

A main hypothesis or approximation of the proposed cohesive damage model is: *the overall damage due to the permanent crack opening is only associated with average hydrostatic stress (spherical) state in an RVE, and the overall damage effect due to the average deviatoric stress can be neglected.*

Based on this hypothesis, the particular damage we are interested in is only susceptible to macro-hydrostatic stress state and we neglect the damage effect due to shear deformation or macro-deviatoric stress states. Based on this assumption and since modes II and III types of remote loading will not contribute to crack opening volume, they are absent in our analysis of material damage, though they definitely contribute surface separation and in general there are cohesive shear forces between two sliding crack surfaces.

From this perspective, different macro-stress states with the same hydrostatic stress tensor form an equivalent class, because their propensity to the damage defined in this paper is the same. Therefore, in order to evaluate damage evolution caused by cohesive micro-crack aggregation, for each equivalent class, one may only need to evaluate damage in an RVE caused by a uniform triaxial tension stress state, and uses it to represent the damage incurred in the RVE for all other remote stress boundary conditions in the same equivalent class.

It should be noted that the damage caused by permanent mode I crack opening under remote hydrostatic stress state may have influence on macro-yielding. Nevertheless, the objective of this paper is not deriving macro-yielding behavior via homogenization of micro-yielding, but studying the overall damage effect due to permanent micro-crack openings on macro-yielding.

2. Average theorem for a cohesive RVE

Since the cohesive crack is not a traction-free defect, we may need to reexamine traditional micro-mechanics averaging theory for traction-free defects in a solid. An averaging theorem for solids containing cohesive defects with constant cohesive traction would be useful for our purpose. Define the macro-stress tensor, Σ_{ij} as the volume average of micro-stress tensor in an RVE (Fig. 1),

$$\Sigma_{ij} := \langle \sigma_{ij} \rangle = \frac{1}{V} \int_V \sigma_{ij} \, \mathrm{d}V \tag{2.1}$$

We first consider the average stress in a three-dimensional (3D) elastic representative volume element with a single penny-shaped Barenblatt–Dugdale crack at the center of the RVE. We adopt the assumption that body force has no effect on material properties. The equilibrium equation inside an RVE takes the form,

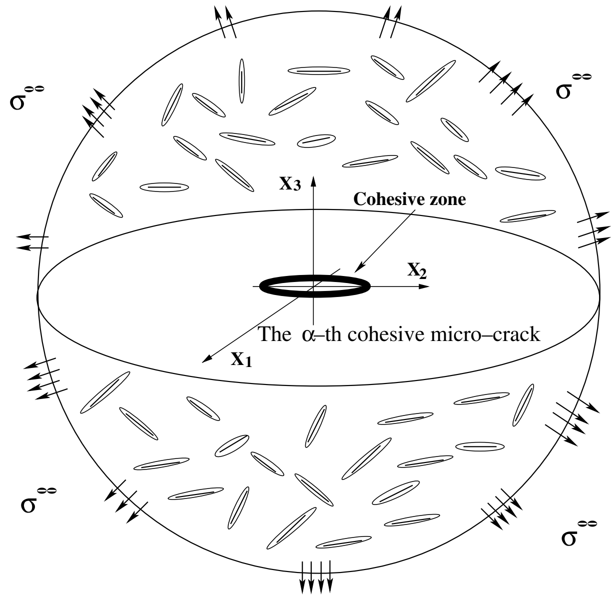

Fig. 1. Isotropic distribution of cracks with different orientations.

$$\sigma_{ji,j} = 0, \quad \forall \mathbf{x} \in V \tag{2.2}$$

Assume that the prescribed tractions on the remote boundary of the RVE (∂V_∞) are generated by a constant stress tensor σ_{ij}^∞. Let ∂V_{ec} denote traction free part of a cohesive crack surface, and let ∂V_{pz} denote the cohesive part of the crack surface where constant traction force t_j is applied. Using divergence theorem, it is straightforward to show that

$$\begin{aligned}
\langle\sigma_{ij}\rangle &= \frac{1}{V}\int_V \sigma_{ij}\,\mathrm{d}V = \frac{1}{V}\int_V (\sigma_{kj}x_i)_{,k}\,\mathrm{d}V \\
&= \frac{1}{V}\left\{\int_V \sigma_{kj}^\infty \delta_{ik}\,\mathrm{d}V - \int_{\partial V_{ec}} 0\cdot x_i n_k\,\mathrm{d}S - \int_{\partial V_{pz}} \sigma_{kj}x_i n_k\,\mathrm{d}S\right\} = \sigma_{ij}^\infty - \frac{1}{V}\int_{\partial V_{pz}} \sigma_{kj}x_i n_k\,\mathrm{d}S \\
&= \sigma_{ij}^\infty - \frac{1}{V}\int_{\partial V_{pz}} t_j x_i\,\mathrm{d}S
\end{aligned} \tag{2.3}$$

where t_j is the constant cohesive traction.

Note that $\partial V_{pz} = \partial V_{pz+} \cup \partial V_{pz-}$ and $|\partial V_{pz+}| = |\partial V_{pz-}| = \frac{1}{2}|\partial V_{pz}|$, where subscript '+' and '−' are used to denote upper and lower part of the crack surfaces. So the last term in (2.3) becomes

$$\frac{1}{V}\int_{\partial V_{pz}} t_j x_i\,\mathrm{d}S = \frac{1}{V}\left(\int_{\partial V_{pz+}} t_j^+ x_i\,\mathrm{d}S + \int_{\partial V_{pz-}} t_j^- x_i\,\mathrm{d}S\right) = 0 \tag{2.4}$$

where $t_j^+ = -t_j^-$ are the cohesive tractions acting on ∂V_{pz+} and ∂V_{pz-} respectively.

Therefore, the average stress inside the RVE will equal to remote stress

$$\Sigma_{ij} = \langle \sigma_{ij} \rangle = \sigma_{ij}^{\infty} \tag{2.5}$$

Now consider a 3D RVE with N cohesive cracks randomly distributed inside (see Fig. 1). As shown above,

$$\langle \sigma_{ij} \rangle = \sigma_{ij}^{\infty} - \frac{1}{V} \sum_{\alpha=1}^{N} \int_{\partial V_{pz\alpha}} t_j^{(\alpha)} x_i \, \mathrm{d}S = \sigma_{ij}^{\infty} \tag{2.6}$$

Hence, the following averaging theorem holds.

Theorem 2.1. *Suppose*

1. *An elastic representative volume element contains N Barenblatt–Dugdale penny-shaped cracks with cohesive tractions in the cohesive zones*;
2. *The tractions on the remote boundary of the RVE is generated by a constant stress tensor*, *i.e.*, $t_i^{\infty} = n_j \sigma_{ji}^{\infty}$, *and* $\sigma_{ij}^{\infty} = \text{const.}$

The macro-stress tensor of an RVE equals to the remote constant stress tensor, *i.e.*

$$\Sigma_{ij} = \langle \sigma_{ij} \rangle = \sigma_{ij}^{\infty} \tag{2.7}$$

Note that for hydrostatic remote loading,

$$\sigma_{ij}^{\infty} = \sigma^{\infty} \delta_{ij} \tag{2.8}$$

By the averaging theorem, it is obvious that

$$\Sigma_{\mathrm{m}} = \sigma^{\infty} \tag{2.9}$$

where $\Sigma_{\mathrm{m}} = \dfrac{1}{3} \Sigma_{ii}$.

3. Penny-shaped crack under uniform triaxial tension

Before proceeding to homogenize three-dimensional (3D) cohesive crack, we first outline the analytical solution of 3D penny-shaped crack in an RVE that is under uniform triaxial tension (see Fig. 2).

Penny-shaped Dugdale crack problem has been studied by several authors. The early contribution was made by Keer and Mura [21], who used the Tresca yield criterion to link the cohesive strength to micro-yield stress. In their study, only uniaxial tension loading was considered. More recently, Chen and Keer [6,7] re-examined the problem, and they obtained the general solutions

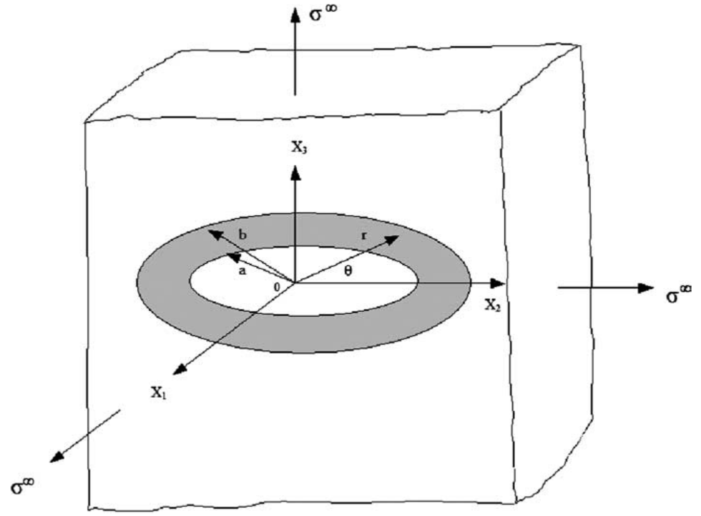

Fig. 2. A penny-shaped cohesive crack in representative volume element (the shaded region: cohesive zone-yielded ring).

for a penny-shaped cohesive crack under mixed-mode loading. On the other hand, however, the problem has not been thoroughly examined from micro-mechanics perspective. For example, the connection among the onset value of cohesive strength, micro-yield stress in an RVE, and remote macro-stress has not been made. By examining a cohesive penny-shaped crack model in an RVE, the study provides a link among cohesive strength, micro-yield stress, and remote stresses on the boundary of an RVE, which provides a foundation for ensuing homogenizations.

3.1. Three-dimensional penny-shaped crack problem

Consider a three-dimensional penny-shaped Dugdale crack of radius a with a ring-shaped cohesive zone with width $b-a$ in an RVE, which may be viewed as an infinite isotropic space by "*a micro-observer*" inside the RVE.

Let the outward normal to crack surface parallel to Z (X_3) axis (see Fig. 2) and a uniform triaxial tension stress is applied at the remote boundary of the RVE, $\sigma_{ij}^{\infty} = \sigma^{\infty}\delta_{ij}$ and $\sigma^{\infty} = \Sigma_{\mathrm{m}}$ based on average theorem shown above. In cylindrical coordinate, the traction conditions on the remote boundary ∂V_{∞} and symmetric displacement boundary condition are expressed as

$$\sigma_{zz}|_{\partial V_{\infty}} = \Sigma_{\mathrm{m}} \tag{3.1}$$

$$\sigma_{rr}|_{\partial V_{\infty}} = \Sigma_{\mathrm{m}} \tag{3.2}$$

$$\sigma_{\theta\theta}|_{\partial V_{\infty}} = \Sigma_{\mathrm{m}} \tag{3.3}$$

$$u_z(r,\theta,0) = 0, \quad b \leqslant r, \;\; 0 \leqslant \theta \leqslant 2\pi \tag{3.4}$$

The stress distribution on the crack surface and cohesive zone is

$$\sigma_{zz}(r,\theta,0) = \sigma_0 H(r-a), \quad 0 \leqslant r \leqslant b, \;\; 0 \leqslant \theta \leqslant 2\pi \tag{3.5}$$

where Σ_{m} is the remote stress, $H(r-a)$ is the Heaviside function, and σ_0 is the material's cohesive strength, the onset value for crack opening, and it is different from the micro-yielding stress. The problem can be solved via superposition of two sub-problems: a trivial problem—an intact RVE in uniform triaxial tension state, i.e. $\forall \mathbf{x} \in V$,

$$\sigma_{zz}^{(0)} = \Sigma_{\mathrm{m}} \tag{3.6}$$

$$\sigma_{rr}^{(0)} = \Sigma_{\mathrm{m}} \tag{3.7}$$

$$\sigma_{\theta\theta}^{(0)} = \Sigma_{\mathrm{m}} \tag{3.8}$$

$$\sigma_{rz}^{(0)} = \sigma_{r\theta}^{(0)} = \sigma_{z\theta}^{(0)} = 0 \tag{3.9}$$

and a crack problem—an RVE with a center crack that is subjected to the following boundary conditions (see Fig. 3).

$$\sigma_{zz}^{(c)}\big|_{\partial V_\infty} = 0 \tag{3.10}$$

$$\sigma_{rr}^{(c)}\big|_{\partial V_\infty} = 0 \tag{3.11}$$

$$\sigma_{\theta\theta}^{(c)}\Big|_{\partial V_\infty} = 0 \tag{3.12}$$

$$\sigma_{zz}^{(c)}(r,\theta,0) = -\Sigma_{\mathrm{m}} + \sigma_0 H(r-a), \quad 0 < r < b, \;\; 0 \leqslant \theta \leqslant 2\pi \tag{3.13}$$

$$u_z^{(c)}(r,\theta,0) = 0, \quad b \leqslant r, \;\; 0 \leqslant \theta \leqslant 2\pi \tag{3.14}$$

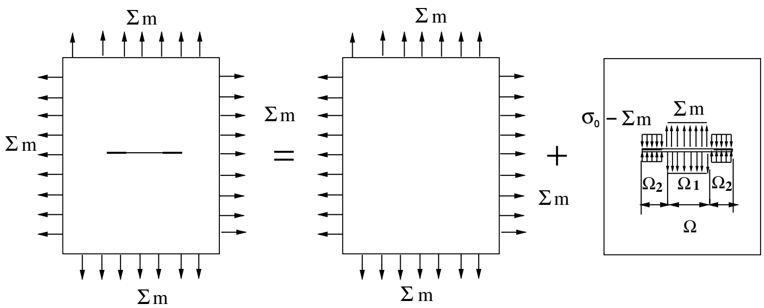

Fig. 3. Illustration of decomposition of cohesive crack problem.

The second problem may be solved by introducing Papkovitch–Neuber displacement potential (see [12,27]). If body force is absent, the displacement fields can be expressed as follows

$$2\mu^* u_r^{(c)} = -(1-2\nu^*)\frac{\partial \Phi}{\partial r} - z\frac{\partial^2 \Phi}{\partial r \partial z} \tag{3.15}$$

$$2\mu^* u_\theta^{(c)} = -(1-2\nu^*)\frac{1}{r}\frac{\partial \Phi}{\partial \theta} - \frac{z}{r}\frac{\partial^2 \Phi}{\partial \theta \partial z} \tag{3.16}$$

$$2\mu^* u_z^{(c)} = 2(1-\nu^*)\frac{\partial \Phi}{\partial z} - z\frac{\partial^2 \Phi}{\partial z^2} \tag{3.17}$$

where the potential function is harmonic, i.e. $\nabla^2 \Phi = 0$; the material constants, shear modulus μ^*, and Poisson's ratio ν^*, are unspecified at the moment, which may depend on the later homogenization procedures. By using kinematic relations and elastic constitutive laws, the stress components can be expressed as

$$\sigma_{rr}^{(c)} = 2\nu^*\frac{\partial^2 \Phi}{\partial z^2} - (1-2\nu^*)\frac{\partial^2 \Phi}{\partial r^2} - z\frac{\partial^3 \Phi}{\partial r^2 \partial z} \tag{3.18}$$

$$\sigma_{\theta\theta}^{(c)} = -\left(2\nu^*\frac{\partial^2 \Phi}{\partial r^2} + \frac{1}{r}\frac{\partial \Phi}{\partial r} + \frac{1}{r^2}\frac{\partial^2 \Phi}{\partial \theta^2} + \frac{z}{r}\frac{\partial^2 \Phi}{\partial r \partial z} + \frac{z}{r^2}\frac{\partial^3 \Phi}{\partial \theta^2 \partial z}\right) \tag{3.19}$$

$$\sigma_{zz}^{(c)} = \frac{\partial^2 \Phi}{\partial z^2} - z\frac{\partial^3 \Phi}{\partial z^3} \tag{3.20}$$

$$\sigma_{zr}^{(c)} = -z\frac{\partial^3 \Phi}{\partial r \partial z^2} \tag{3.21}$$

$$\sigma_{z\theta}^{(c)} = -\frac{z}{r}\frac{\partial^3 \Phi}{\partial \theta \partial z^2} \tag{3.22}$$

$$\sigma_{r\theta}^{(c)} = \frac{1}{r}\left[(1-2\nu^*)\left(\frac{1}{r}\frac{\partial \Phi}{\partial \theta} - \frac{\partial^2 \Phi}{\partial \theta \partial r}\right) + z\left(\frac{1}{r}\frac{\partial^2 \Phi}{\partial \theta \partial z} - \frac{\partial^3 \Phi}{\partial \theta \partial r \partial z}\right)\right] \tag{3.23}$$

The solution of the harmonic potential function, Φ can be sought by using Hankel transformation. Define the symmetric mode (zero-order) Hankel transform,

$$\begin{cases} \bar{\Phi}(\xi, z) := \int_0^\infty r\Phi(r,z)J_0(\xi r)\,\mathrm{d}r \\ \Phi(r,z) := \int_0^\infty \xi\bar{\Phi}(\xi,z)J_0(\xi r)\,\mathrm{d}\xi \end{cases} \tag{3.24}$$

where $J_0(\xi z)$ is zero-order Bessel function. The Laplace equation can be reduced to an ordinary differential equation

$$\nabla^2 \Phi = 0 \Rightarrow \frac{\partial^2 \bar{\Phi}}{\partial z^2} - \xi^2 \bar{\Phi} = 0 \tag{3.25}$$

By considering the remote boundary condition, $\bar{\Phi}(\xi, z) \to 0$ as $z \to 0$, and the solution of (3.25) is

$$\bar{\Phi}(\xi, z) = \mathscr{A}(\xi)\exp(-\xi z) \tag{3.26}$$

Substitute (3.26) into $(3.24)_2$. The displacement potential may be expressed as

$$\Phi(r, z) = -\int_0^\infty \xi^{-1} A(\xi)\exp(-\xi z) J_0(\xi r)\, \mathrm{d}\xi \tag{3.27}$$

where $A(\xi) = -\mathscr{A}(\xi)\xi^2$, which is an unknown function to be determined. The boundary conditions (3.13) and (3.14) render the following dual integral equations

$$\begin{cases} \int_0^\infty \xi A(\xi) J_0(\xi r)\, \mathrm{d}\xi = \Sigma_{\mathrm{m}} - \sigma_0 H(r-a), & 0 < r < b \\ \int_0^\infty A(\xi) J_0(\xi r)\, \mathrm{d}\xi = 0, & r \geqslant b \end{cases} \tag{3.28}$$

Choose $A(\xi)$ the following form

$$A(\xi) = \int_0^b \phi(t) \sin \xi t\, \mathrm{d}t \tag{3.29}$$

One may verify that $(3.28)_2$ is automatically satisfied.

Solving the first equation of $(3.28)_1$, one may find that

$$\phi(t) = \begin{cases} \dfrac{2}{\pi}\Sigma_{\mathrm{m}} t & t < a \\ \dfrac{2}{\pi}(\Sigma_{\mathrm{m}} t - \sigma_0\sqrt{t^2 - a^2}) & a < t < b \end{cases} \tag{3.30}$$

and hence $A(\xi)$ and $\Psi(r, z)$.

With the solution of potential function Ψ at hand, stress components (3.18)–(3.23) can be determined. After lengthy calculation, one may find that in the yield ring ($z = 0$ and $a < r < b$) the stress distributions are

$$\sigma_{zz}^{(c)} = \sigma_0 - \Sigma_{\mathrm{m}} \tag{3.31}$$

$$\sigma_{rr}^{(c)} = -\frac{1 + 2\nu^*}{2}\Sigma_{\mathrm{m}} + \left[\frac{1 - 2\nu^*}{2}\left(1 + \frac{a^2}{r^2}\right) + 2\nu^*\right]\sigma_0 \tag{3.32}$$

$$\sigma_{\theta\theta}^{(c)} = -\frac{1 + 2\nu^*}{2}\Sigma_{\mathrm{m}} + \left[\frac{1 - 2\nu^*}{2}\left(1 - \frac{a^2}{r^2}\right) + 2\nu^*\right]\sigma_0 \tag{3.33}$$

$$\sigma_{rz}^{(c)} = \sigma_{r\theta}^{(c)} = \sigma_{z\theta}^{(c)} = 0 \tag{3.34}$$

To ensure the stresses at crack tip to be finite, the size of the cohesive zone, a/b, remote stress Σ_{m}, and the cohesive stress, σ_0 are related through the following expression,

$$\frac{a}{b} = \sqrt{1 - \frac{(\Sigma_{\mathrm{m}})^2}{(\sigma_0)^2}} \quad \text{or} \quad \frac{\Sigma_{\mathrm{m}}}{\sigma_0} = \sqrt{1 - \frac{a^2}{b^2}} \tag{3.35}$$

If we are mainly interested in inelastic deformation of quasi-brittle materials, we may assume that micro-scale yielding due to hydrostatic stress state is small-scale yielding: $\frac{a^2}{b^2} \approx 1$. Therefore, $(\frac{a^2}{r^2} \approx 1)$, for $a \leqslant r \leqslant b$. The total stress distribution within the cohesive zone (3.31)–(3.34) may be approximated as

$$\sigma_{zz}^{(t)} = \sigma_{zz}^{(0)} + \sigma_{zz}^{(c)} = \sigma_0 \tag{3.36}$$

$$\sigma_{rr}^{(t)} = \sigma_{rr}^{(0)} + \sigma_{rr}^{(c)} = \frac{1-2v^*}{2}\Sigma_{\mathrm{m}} + \sigma_0 \tag{3.37}$$

$$\sigma_{\theta\theta}^{(t)} = \sigma_{\theta\theta}^{(0)} + \sigma_{\theta\theta}^{(c)} = \frac{1-2v^*}{2}\Sigma_{\mathrm{m}} + 2v^*\sigma_0 \tag{3.38}$$

$$\sigma_{rz}^{(t)} = \sigma_{r\theta}^{(t)} = \sigma_{z\theta}^{(t)} = 0 \tag{3.39}$$

It is assumed that inside the cohesive zone micro-plastic yielding is controlled by the Huber–von Mises criterion. Therefore, we can link the cohesive strength, σ_0, with the yield stress of the virgin material, σ_{Y}, by

$$\frac{1}{2}\left[\left(\sigma_{rr}^{(t)} - \sigma_{zz}^{(t)}\right)^2 + \left(\sigma_{\theta\theta}^{(t)} - \sigma_{zz}^{(t)}\right)^2 + \left(\sigma_{rr}^{(t)} - \sigma_{\theta\theta}^{(t)}\right)^2\right] = \sigma_{\mathrm{Y}}^2 \tag{3.40}$$

Substitute Eqs. (3.36)–(3.38) into (3.40) and solve for σ_0. The following quadratic equation may be obtained

$$4\left(\frac{\sigma_0}{\Sigma_{\mathrm{m}}}\right)^2 - 2\left(\frac{\sigma_0}{\Sigma_{\mathrm{m}}}\right) + 1 - \left(\frac{2}{1-2v^*}\frac{\sigma_{\mathrm{Y}}}{\Sigma_{\mathrm{m}}}\right)^2 = 0 \tag{3.41}$$

which has two roots. The positive root is chosen to link the cohesive stress σ_0 with the yield stress in uniaxial tension σ_{Y},

$$\frac{\sigma_0}{\Sigma_{\mathrm{m}}} = \frac{1 + \sqrt{\left(\frac{4}{1-2v^*}\frac{\sigma_{\mathrm{Y}}}{\Sigma_{\mathrm{m}}}\right)^2 - 3}}{4} \tag{3.42}$$

3.2. Crack opening displacement

Consider the displacement at crack surface (Eq. (3.17) ($z = 0$)),

$$u_z(r) = \frac{(1-\nu^*)}{\mu^*}\frac{\partial \Phi}{\partial z} = \frac{1-\nu^*}{\mu^*}\int_r^b \frac{\phi(t)}{\sqrt{t^2-r^2}}\,\mathrm{d}t$$
$$= \begin{cases} \dfrac{2}{\pi}\left(\dfrac{1-\nu^*}{\mu^*}\right)\left(\Sigma_{\mathrm{m}}\sqrt{b^2-r^2} - \sigma_0\displaystyle\int_a^b \frac{\sqrt{t^2-a^2}}{\sqrt{t^2-r^2}}\,\mathrm{d}t\right) & 0 < r < a \\ \dfrac{2}{\pi}\left(\dfrac{1-\nu^*}{\mu^*}\right)\left(\Sigma_{\mathrm{m}}\sqrt{b^2-r^2} - \sigma_0\displaystyle\int_r^b \frac{\sqrt{t^2-a^2}}{\sqrt{t^2-r^2}}\,\mathrm{d}t\right) & a < r < b \end{cases} \tag{3.43}$$

Denote the traction-free crack surface as $\partial V_{ec} = \partial V_{ec+} \cup \partial V_{ec-}$ and its projection onto X_1X_2 plane as Ω_1. Denote the surface of the cohesive zone (ring shape) as $\partial V_{pz} = \partial V_{pz+} \cup \partial V_{pz-}$ and its projection onto X_1X_2 plane as Ω_2. Hence, $\Omega = \Omega_1 \cup \Omega_2$ (see Fig. 4).

Define displacement jump,

$$[u_z] = u_z^+ - u_z^- = 2u_z \tag{3.44}$$

The volume of crack opening over Ω_1 is

$$\int_{\Omega_1}[u_z]\,\mathrm{d}A = \frac{8(1-\nu^*)}{\mu^*}\left(\Sigma_{\mathrm{m}}\int_0^a \sqrt{b^2-r^2}\,r\,\mathrm{d}r - \sigma_0\int_0^a\int_a^b \frac{\sqrt{t^2-a^2}}{\sqrt{t^2-r^2}}\,r\,\mathrm{d}t\,\mathrm{d}r\right)$$
$$= \frac{8(1-\nu^*)}{3\mu^*}\left\{\Sigma_{\mathrm{m}}\left[b^3 - (b^2-a^2)^{\frac{3}{2}}\right] - \sigma_0\left[(b^2-a^2)^{\frac{3}{2}} - (b^3 - 3a^2b + 2a^3)\right]\right\} \tag{3.45}$$

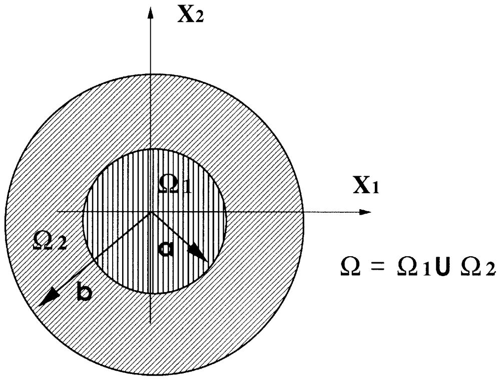

Fig. 4. Projection domain of crack surface and cohesive zone.

The volume of crack opening over the yielding ring $\Omega_2 (a < r < b)$ is

$$\int_{\Omega_2} [u_z]\,\mathrm{d}A = \frac{8(1-\nu^*)}{\mu^*}\left[\Sigma_{\mathrm{m}}\int_a^b \sqrt{b^2-r^2}\,r\,\mathrm{d}r - \sigma_0\int_a^b\int_r^b \frac{\sqrt{t^2-a^2}}{\sqrt{t^2-r^2}}\,r\,\mathrm{d}t\,\mathrm{d}r\right]$$
$$= \frac{8(1-\nu^*)}{3\mu^*}\left[\Sigma_{\mathrm{m}}(b^2-a^2)^{\frac{3}{2}} - \sigma_0(b^3-3a^2b+2a^3)\right] \tag{3.46}$$

The total volume of crack opening by a single cohesive crack is the integration of crack opening displacement over the entire projection area, $\Omega = \Omega_1 \cup \Omega_2$. With the aid of (3.45), (3.46), and (3.35), it is readily to show that

$$V_{\mathrm{c}} = \int_{\Omega} [u_z]\,\mathrm{d}A = \int_{\Omega_1} [u_z]\,\mathrm{d}A + \int_{\Omega_2} [u_z]\,\mathrm{d}A = \frac{8(1-\nu^*)}{3\mu^*} b^3\left[\Sigma_{\mathrm{m}} - \sigma_0\left(1-\left(\frac{a}{b}\right)^2\right)^{\frac{3}{2}}\right]$$
$$= \frac{8(1-\nu^*)a^3}{3\mu^*}\frac{\Sigma_{\mathrm{m}}}{\sqrt{1-\left(\frac{\Sigma_{\mathrm{m}}}{\sigma_0}\right)^2}} \tag{3.47}$$

4. Effective elastic material properties of an RVE

Define the *macro-strain tensor*

$$\mathscr{E}_{ij} := \frac{\partial \bar{W}_{\mathrm{c}}}{\partial \Sigma_{ij}} =: \bar{D}_{ijk\ell}\Sigma_{k\ell} = \bar{D}_{ijk\ell}\sigma^{\infty}_{k\ell} \tag{4.1}$$

where $\bar{W}_{\mathrm{c}}$ is the overall complementary energy density of an RVE. $\Sigma_{ij} := \langle\sigma_{ij}\rangle$ is the macro-stress tensor defined previously, and $\bar{D}_{ijk\ell}$ is the effective compliance moduli.

Note that the macro-strain in an RVE may not be the volume average strain in an RVE, that is $\mathscr{E}_{ij} \neq \langle\epsilon_{ij}\rangle$. Furthermore Eq. (4.1) may not be a linear relationship, because $\bar{D}_{ijk\ell}$ depend on Σ_{ij} in general.

A common strategy for homogenization of randomly distributed defects is to find a so-called additional strain tensor, $\boldsymbol{\epsilon}^{(\mathrm{add})}$ (e.g. [30,31,34]), such that

$$\mathscr{E}_{ij} = \epsilon^{(0)}_{ij} + \epsilon^{(\mathrm{add})}_{ij} \tag{4.2}$$

where $\epsilon^{(0)}_{ij} = D_{ijk\ell}\Sigma_{k\ell}$ and $D_{ijk\ell}$ is the elastic compliance of the corresponding virgin material.

If the relationship between additional strain and macro-stress can be found, $\epsilon^{(\mathrm{add})}_{ij} = H_{ijk\ell}\Sigma_{k\ell}$, where $H_{ijk\ell}$ is the added compliance due to micro-cracks, subsequently the effective elastic compliance moduli, $\bar{\mathbf{D}}$, can be deduced.

For an elastic solid containing a traction-free crack, the additional strain can be calculated by using Hill's formula [16,19]

$$\boldsymbol{\epsilon}^{(\mathrm{add})} = \frac{1}{2V}\int_{\Omega}(\mathbf{n}\otimes[\mathbf{u}] + [\mathbf{u}]\otimes\mathbf{n})\,\mathrm{d}S \tag{4.3}$$

However, Hill's formula may not be applicable in homogenizations of cohesive cracks, because of the presence of nonzero tractions in the cohesive zone.

To find an additional strain formula for cohesive cracks, we resort to energy methods. The essence of energy methods is to find the energy release in a cohesive fracture process and hence to find the equivalent reduction of material properties. Nonetheless, the energy dissipation process in cohesive fracture is much more complicated than a purely elastic fracture process. It includes energy dissipation from both surface separation and plastic dissipation. We first study the average energy release rate of an RVE with distributed cohesive micro-cracks subjected to uniform triaxial loading $\sigma_{ij}^{\infty} = \Sigma_{\rm m}\delta_{ij}$.

4.1. Average energy release rate

To estimate energy loss during a damage process requires an in-depth understanding of the physical process involved. However, sensible estimates may be made based on simplified assumptions.

In the first estimate, we assume that the energy release during a cohesive damage process comes solely from traction-free surface separation, which may be estimated by using J-integral [36]. The J-integral of a Dugdale crack has been calculated by Rice [36,37],

$$J = \sigma_0 \delta_t \tag{4.4}$$

where δ_t is the so-called crack tip opening displacement (CTOD). The 3D penny shape Dugdale crack tip opening displacement is also given by Rice [37],

$$\delta_t = \frac{4}{\pi}\left(\frac{1-\nu^*}{\mu^*}\right) a\sigma_0 \left(1 - \sqrt{1 - \left(\frac{\Sigma_{\rm m}}{\sigma_0}\right)^2}\right) \tag{4.5}$$

which can be also verified through Eq. (3.43). Hence

$$J = \sigma_0 \delta_t = \frac{4}{\pi}\left(\frac{1-\nu^*}{\mu^*}\right) a\sigma_0^2 \left(1 - \sqrt{1 - \left(\frac{\Sigma_{\rm m}}{\sigma_0}\right)^2}\right) \tag{4.6}$$

In order to link the J-integral (energy release rate) to the energy release due surface separation, the energy release due to crack growth, $\mathscr{R}_1$, can be first related with the so-called M-integral (see: [4,5]),

$$M = \int\int_S \left\{ W\mathbf{x}\cdot\mathbf{n} - [(\mathbf{x}\cdot\nabla)\mathbf{u}]\cdot\mathbf{t} - \frac{1}{2}\mathbf{t}\cdot\mathbf{u} \right\} {\rm d}S \tag{4.7}$$

where $\mathbf{x}$ is the position vector, $\mathbf{u}$ is the displacement, $\mathbf{n}$ is the unit outward normal to S, W is the strain energy density, and ∇ is the gradient operator. Note that the surface S completely encloses the crack (see Fig. 5), and it consists of two planes coincident with the traction-free surfaces and a tunnel that surrounds the crack front C.

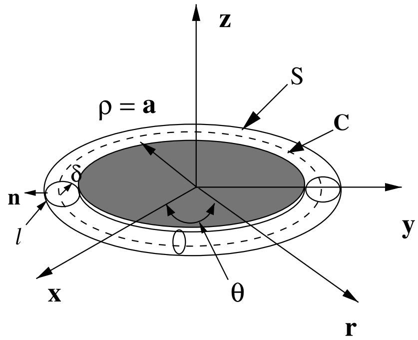

Fig. 5. Surface S surrounding a penny-shaped crack front C.

Since $\mathbf{x}\cdot\mathbf{n}=0$ and $\mathbf{t}=0$ on the traction-free surface, the expression for M-integral becomes

$$M=\oint_c \rho(s)\lim_{\delta\to 0}\oint_\ell\left(Wn_r-\boldsymbol{\sigma}\cdot\frac{\partial\mathbf{u}}{\partial r}\right)\mathrm{d}\ell\,\mathrm{d}S-\int\int_S\frac{1}{2}\mathbf{t}\cdot\mathbf{n}\mathrm{d}S=\oint_c \rho J\,\mathrm{d}S \tag{4.8}$$

where n_r is the rth component of unit outnormal vector $\mathbf{n}$.

The term $\frac{1}{2}\int\int_S \mathbf{t}\cdot\mathbf{n}\,\mathrm{d}S=0$ in (4.8) vanishes as $\delta\to 0$. The integrand inside the outer integral of (4.8) becomes the familiar J-integral. Budiansky and Rice [4] interpreted the M-integral of (4.8) as the energy release rate associated with self-similar growth of a crack, in which each point of C recedes radially from the origin at a rate proportional to its distance therefrom. For penny-shaped cracks, one may choose $\rho=a$ and $\mathrm{d}S=a\,\mathrm{d}\theta$ (see Fig. 5), and it therefore yields the following expression,

$$\begin{aligned}M=a\frac{\partial\mathscr{R}_1}{\partial a}=\oint_c\rho J\,\mathrm{d}S&=\int_0^{2\pi}\frac{4}{\pi}\left(\frac{1-\nu^*}{\mu^*}\right)a^3\sigma_0^2\left(1-\sqrt{1-\left(\frac{\Sigma_{\mathrm{m}}}{\sigma_0}\right)^2}\right)\mathrm{d}\theta\\&=\frac{8(1-\nu^*)}{\mu^*}\sigma_0^2\left(1-\sqrt{1-\left(\frac{\Sigma_{\mathrm{m}}}{\sigma_0}\right)^2}\right)a^3\end{aligned} \tag{4.9}$$

The energy release due to traction-free surface separation is then,

$$\mathscr{R}_1=\frac{8(1-\nu^*)}{3\mu^*}\sigma_0^2a^3\left(1-\sqrt{1-\left(\frac{\Sigma_{\mathrm{m}}}{\sigma_0}\right)^2}\right) \tag{4.10}$$

Remark 4.1

1. In the procedure of deriving the energy release from M-integral, we assume the ratio of b/a, or the ratio of $\Sigma_{\mathrm{m}}/\sigma_0$, is kept constant during crack extension;
2. For cohesive cracks, the total energy release due to the total crack surface separation or damage consumption is a complicated issue. For solids containing cohesive defects, J integral may not

be interpreted as the total energy release rate, since the involvement of plastic dissipation in the cohesive zone. A related discussion can be also found in [28,33,42]. However, under the assumption of small scale yielding, the above approximation may be accepted as "the conventional wisdom". The energy release due to traction-free surface separation provides a lower bound for estimation of energy consumption in the damage process.

Since the energy release due to traction-free surface separation, $\mathscr{R}_1$, is only part of the total energy release, in the second estimate, an upper bound solution is sought to evaluate energy release contribution to damage process. In the second estimate, we assume that the total energy release of a cohesive crack is completely consumed in surface separation, which may or may not be true in cohesive fracture, because of plastic dissipation in the cohesive zone.

The total energy release of a 3D penny-shaped crack can be calculated as

$$\mathscr{R}_2 = \int_{\Omega} \Sigma_{\mathrm{m}}[u_z]\,\mathrm{d}S - \int_{\Omega_2} \sigma_0[u_z]\,\mathrm{d}S = \frac{16(1-v^*)}{3\mu^*}\sigma_0^2 a^3\left(1-\sqrt{1-\left(\frac{\Sigma_{\mathrm{m}}}{\sigma_0}\right)^2}\right) \tag{4.11}$$

Interestingly, one may find that $\mathscr{R}_2 = 2\mathscr{R}_1$. We then can express the two estimates in a unified fashion,

$$\mathscr{R}_\omega = \frac{8\omega(1-v^*)}{3\mu^*}\sigma_0^2 a^3\left(1-\sqrt{1-\left(\frac{\Sigma_{\mathrm{m}}}{\sigma_0}\right)^2}\right), \quad \omega = 1,2 \tag{4.12}$$

Consider that there are N penny-shaped cracks inside the RVE, and define the crack opening volume fraction as

$$f := \sum_{\alpha=1}^{N} \frac{4\pi a_\alpha^3}{3V}\beta, \tag{4.13}$$

where a_α is the radius of the αth crack, and $4\pi a_\alpha^3/3$ is the volume of a sphere with radius a_α, and β is the ratio between the volume of permanent crack opening and the volume of total crack opening of a cohesive crack. For simplicity, we assume that this ratio is fixed for every crack inside an RVE. Obviously, $0 \leqslant \beta \leqslant 1$.

Utilizing (4.12) and (4.13), the density of energy release estimate can be written as

$$\begin{aligned}\frac{\mathscr{R}_\omega}{V} &= \frac{8\omega(1-v^*)}{3\mu^*\beta}\sigma_0^2\sum_{\alpha=1}^{N}\left(\frac{4\pi a_\alpha^3}{3V}\beta\right)\frac{3}{4\pi}\left(1-\sqrt{1-\left(\frac{\Sigma_{\mathrm{m}}}{\sigma_0}\right)^2}\right)\\ &= \frac{2\omega(1-v^*)}{\beta\pi\mu^*}\sigma_0^2 f\left(1-\sqrt{1-\left(\frac{\Sigma_{\mathrm{m}}}{\sigma_0}\right)^2}\right), \quad \omega = 1,2\end{aligned} \tag{4.14}$$

The overall complementary energy density may then be expressed as the sum of complementary energy density of corresponding virgin material and the density of energy release due to micro-crack distribution,

$$\bar{W}^c = W^c + \frac{\mathscr{R}_\omega}{V} = \frac{1}{2} D_{ijk\ell}\sigma^\infty_{ij}\sigma^\infty_{k\ell} + \frac{2\omega(1-\nu^*)}{\beta\pi\mu^*}\sigma_0^2 f\left(1-\sqrt{1-\left(\frac{\Sigma_\mathrm{m}}{\sigma_0}\right)^2}\right), \quad \omega = 1,2 \tag{4.15}$$

Based on definition (4.1) and the averaging Theorem 2.1, for a given crack opening volume fraction, f, the macro-strain tensor can be obtained as

$$\mathscr{E}_{ij} = \frac{\partial \bar{W}^c}{\partial \Sigma_{ij}} = \frac{\partial \bar{W}^c}{\partial \sigma^\infty_{ij}} = D_{ijk\ell}\sigma^\infty_{k\ell} + \frac{\partial(\mathscr{R}_\omega/V)}{\partial \Sigma_\mathrm{m}}\frac{\partial \Sigma_\mathrm{m}}{\partial \sigma^\infty_{ij}} = D_{ijk\ell}\sigma^\infty_{k\ell} + \frac{2\omega(1-\nu^*)}{3\beta\pi\mu^*} f \frac{\Sigma_\mathrm{m}\delta_{ij}}{\sqrt{1-\left(\frac{\Sigma_\mathrm{m}}{\sigma_0}\right)^2}} \tag{4.16}$$

It may be noted that Eq. (4.16) is only valid when the RVE is under hydrostatic stress state, i.e., $\sigma^\infty_{ij} = \Sigma_\mathrm{m}\delta_{ij}$. From (4.16), one can find an expression for additional strain

$$\epsilon^{(\mathrm{add})}_{ij} = \frac{2\omega(1-\nu^*)}{3\beta\pi\mu^*} f \frac{\Sigma_\mathrm{m}\delta_{ij}}{\sqrt{1-\left(\frac{\Sigma_\mathrm{m}}{\sigma_0}\right)^2}}, \quad \omega = 1,2 \tag{4.17}$$

4.2. Self-consistent homogenization

A bona fide self-consistent scheme should take into account micro-crack interaction (see [5,17,18]). Since the micro-crack distribution is isotropic, the damaged RVE should also be considered as isotropic *at micro-level*. The micro-crack interaction effect could be captured by taking $\mu^* = \bar{\mu}$ and $\nu^* = \bar{\nu}$ in all above derivations, where $\bar{\mu}$ and $\bar{\nu}$ are effective shear modulus and effective Poisson's ratio in an RVE. Recast Eq. (4.17) into a more general form,

$$\boldsymbol{\epsilon}^{(\mathrm{add})} = \mathbf{H} : \boldsymbol{\Sigma}, \tag{4.18}$$

so

$$\mathscr{E} = \bar{\mathbf{D}} : \boldsymbol{\Sigma} = (\mathbf{D} + \mathbf{H}) : \boldsymbol{\Sigma}, \quad \text{where } \bar{\mathbf{D}} = \mathbf{D} + \mathbf{H} \tag{4.19}$$

where $\mathbf{H}$ is an isotropic tensor, which may be written as

$$\mathbf{H} = \frac{h_1}{3}\mathbf{1}^{(2)} \otimes \mathbf{1}^{(2)} + h_2 \mathbf{1}^{(4s)} \tag{4.20}$$

where $\mathbf{1}^{(2)} = \delta_{ij}\mathbf{e}_i \otimes \mathbf{e}_j$, and $\mathbf{1}^{(4s)} = \frac{1}{2}(\delta_{ik}\delta_{j\ell} + \delta_{i\ell}\delta_{jk})\mathbf{e}_i \otimes \mathbf{e}_j \otimes \mathbf{e}_k \otimes \mathbf{e}_\ell$, and parameters h_1, h_2 are yet to be determined.

Decompose

$$\mathbf{D} = \frac{1}{3K}\mathbf{E}^1 + \frac{1}{2\mu}\mathbf{E}^2 \tag{4.21}$$

$$\bar{\mathbf{D}} = \frac{1}{3\bar{K}}\mathbf{E}^1 + \frac{1}{2\bar{\mu}}\mathbf{E}^2 \tag{4.22}$$

$$\mathbf{H} = (h_1 + h_2)\mathbf{E}^1 + h_2\mathbf{E}^2 \tag{4.23}$$

where $\mathbf{E}^1 := \frac{1}{3}\mathbf{1}^{(2)} \otimes \mathbf{1}^{(2)}$, $\mathbf{E}^{(2)} := -\frac{1}{3}\mathbf{1}^{(2)} \otimes \mathbf{1}^{(2)} + \mathbf{1}^{(4s)}$ and consider

$$\frac{1}{3K} = \frac{(1-2v)}{E} \quad \text{and} \quad \frac{1}{3\bar{K}} = \frac{(1-2\bar{v})}{\bar{E}} \tag{4.24}$$

$$\frac{1}{2\mu} = \frac{(1+v)}{E} \quad \text{and} \quad \frac{1}{2\bar{\mu}} = \frac{(1+\bar{v})}{\bar{E}} \tag{4.25}$$

The $\mathbf{H}$ tensor in Eq. (4.20) can not be uniquely determined, since on the remote boundary of the RVE, the traction stress state is hydrostatic, $\mathbf{\Sigma} = \Sigma_{\mathrm{m}}\delta_{ij}\mathbf{e}_i \otimes \mathbf{e}_j$. Hence the information carried in (4.19) only admits one scalar equation,

$$\bar{\mathbf{D}} : (\Sigma_{\mathrm{m}}\delta_{ij}\mathbf{e}_i \otimes \mathbf{e}_j) = (\mathbf{D} + \mathbf{H}) : (\Sigma_{\mathrm{m}}\delta_{ij}\mathbf{e}_i \otimes \mathbf{e}_j) \tag{4.26}$$

Consider $\mathscr{E}_{ij} = \epsilon_{ij}^{(0)} + \epsilon_{ij}^{(\mathrm{add})}$ and identities, $\mathbf{E}^1 : \mathbf{1}^{(2)} = \mathbf{1}^{(2)}$ and $\mathbf{E}^2 : \mathbf{1}^{(2)} = \mathbf{0}$, and by virtue of (4.17) and (4.26), it can be shown that

$$\frac{1}{3\bar{K}} = \frac{1}{3K} + (h_1 + h_2) = \frac{1}{3K} + \frac{2\omega(1-\bar{v})}{3\beta\pi\bar{\mu}} \frac{f}{\sqrt{1 - \left(\frac{\Sigma_{\mathrm{m}}}{\sigma_0}\right)^2}} \tag{4.27}$$

There are two unknowns, $\bar{K}$ and $\bar{\mu}$, or equivalently h_1 and h_2 in Eq. (4.27). Additional condition is needed to uniquely determine $\bar{\mathbf{D}}$ or $\mathbf{H}$. Impose a restriction

$$\frac{\bar{K}}{K} = \frac{\bar{\mu}}{\mu} \tag{4.28}$$

This restriction guarantees the positive definiteness of the overall strain energy. It also implies that the relative reduction of the shear modulus is the same as that of the bulk modulus.

Consider (4.24) and (4.25). A direct consequence of (4.28) is $\bar{v} = v$, which leads

$$\frac{1}{3\bar{K}} = \frac{1}{2\bar{\mu}}\left(\frac{1-2\bar{v}}{1+\bar{v}}\right) = \frac{1}{2\bar{\mu}}\left(\frac{1-2v}{1+v}\right)$$

$$\frac{1}{3\bar{K}} = \frac{1}{2\bar{\mu}}\left(\frac{1-2v}{1+v}\right)$$

which, when substituted into (4.27), leads to the estimates of effective elastic moduli

$$\frac{\bar{K}}{K} = \frac{\bar{\mu}}{\mu} = 1 - \frac{4\omega(1-v^2)}{3\beta\pi(1-2v)} \frac{f}{\sqrt{1-\left(\frac{\Sigma_{\mathrm{m}}}{\sigma_0}\right)^2}}, \quad \omega = 1,2 \tag{4.29}$$

5. Micro-cohesive crack damage models

Before proceeding to construct cohesive damage model, a few definitions are in order. Define the macro-deviatoric stress tensor and its second invariant as

$$\Sigma'_{ij} = \Sigma_{ij} - \tfrac{1}{3}\Sigma_{kk}\delta_{ij} \tag{5.1}$$

$$J_2 = \tfrac{1}{2}\Sigma'_{ij}\Sigma'_{ij} \tag{5.2}$$

Define macro-deviatoric elastic strain tensor, and its second invariant as

$$\mathscr{E}'_{ij} = \frac{1}{2\bar{\mu}}\Sigma'_{ij} \tag{5.3}$$

$$\mathscr{I}_2 = \frac{1}{2}\mathscr{E}'_{ij}\mathscr{E}'_{ij}. \tag{5.4}$$

Homogenization of nonlinear problems is often difficult. Without proper statistical closure, averaging along may not be sufficient to provide sensible results. In this paper, we postulate that there is a limit for the amount of distortional energy that a given material ensemble can store. This reflects in the following hypothesis on the condition of macro-yielding:

Hypothesis 5.1. The macroscopic yielding of an RVE begins when the distortional strain energy density of an RVE

$$U_d := \int_0^{\mathscr{E}'_{ij}} \widetilde{\Sigma}'_{ij}\, \mathrm{d}\widetilde{\mathscr{E}}'_{ij} \tag{5.5}$$

reaches to a threshold. In other words, the maximum elastic distortional energy of an RVE is a material constant,

$$U_d \leqslant U_d^{(\mathrm{cr})}. \tag{5.6}$$

Remark 5.1

1. The postulate is an assumed statistical closure, and it is not based on either micro-mechanics principles, nor experimental results. In other words, the premised condition is a pre-requisite property assigned to all the RVEs in the material that is under investigation.
2. When we study effective elastic material properties, only hydrostatic stress state is applied on the remote boundary of an RVE. Nevertheless, most remote stress states in an equivalent class have nontrivial average deviatoric stress state, i.e. $J_2 \neq 0$.
3. From Eqs. (5.2)–(5.4), one can easily show that

$$\sqrt{J_2} = 2\bar{\mu}\sqrt{\mathscr{I}_2} \tag{5.7}$$

Since the relationship (4.1) and (5.7) are nonlinear in general,

$$U_d \neq \frac{1}{2\bar{\mu}} J_2 \tag{5.8}$$

Interestingly, if the effective shear modulus only depends on the ratio $\Sigma_{\mathrm{m}}/\sigma_0$, i.e. $\bar{\mu} = \bar{\mu}(\Sigma_{\mathrm{m}}/\sigma_0)$, and the ratio $\Sigma_{\mathrm{m}}/\sigma_0$ is independent from $\mathscr{I}_2$, it can be shown that

$$\begin{aligned} U_d &= \int_0^{\mathscr{E}'_{ij}} \widetilde{\Sigma}'_{ij}\,\mathrm{d}\widetilde{\mathscr{E}}'_{ij} = \int_0^{\mathscr{E}'_{ij}} 2\bar{\mu}(\Sigma_{\mathrm{m}}/\sigma_0)\widetilde{\mathscr{E}}'_{ij}\,\mathrm{d}\widetilde{\mathscr{E}}'_{ij} = \int_0^{\mathscr{I}_2} 2\bar{\mu}(\Sigma_{\mathrm{m}}/\sigma_0)\,\mathrm{d}\mathscr{I}_2 \\ &= 2\bar{\mu}(\Sigma_{\mathrm{m}}/\sigma_0)\mathscr{I}_2 = \frac{1}{2\bar{\mu}} J_2 \end{aligned} \tag{5.9}$$

4. Eq. (5.6) is a reminiscence of the Hencky's maximum distortional energy principle in traditional infinitesimal plasticity. According to Hencky's maximum distortional energy theory [15], the threshold of yielding for a material point can be measured by its ability to absorb certain amount of elastic distortional energy density. However, the elastic distortional energy density of an RVE does not equal to the average elastic distortional energy density, i.e.

$$U_d = \int_0^{\mathscr{E}'_{ij}} \widetilde{\Sigma}'_{ij}\,\mathrm{d}\widetilde{\mathscr{E}}'_{ij} \neq \frac{1}{V}\int_V \int_0^{\epsilon'_{ij}} \tilde{\sigma}'_{ij}\,\mathrm{d}\tilde{\epsilon}'_{ij}\,\mathrm{d}V \tag{5.10}$$

In other words

$$\int_0^{\mathscr{E}'_{ij}} \langle\sigma_{ij}\rangle'\,\mathrm{d}\langle\epsilon^e_{ij}\rangle' \neq \frac{1}{2}\langle\sigma'_{ij}\epsilon'_{ij}\rangle \tag{5.11}$$

5. The criterion can be calibrated in an uniaxial tension test of the virgin material

$$U_d^{(\mathrm{cr})} = \frac{1}{6\mu}\sigma_{\mathrm{Y}}^2 \tag{5.12}$$

In a real damage evolution process, the above criteria take the following form

$$U_d = \frac{\Sigma_{\mathrm{eq}}^2}{6\bar{\mu}} \leqslant U_d^{(\mathrm{cr})}, \quad \text{where } \Sigma_{\mathrm{eq}} := \sqrt{3J_2} \tag{5.13}$$

Then the criterion of the maximum distortional energy density of an RVE becomes

$$\frac{\Sigma_{\rm eq}^2}{\sigma_{\rm Y}^2} = \frac{\bar{\mu}}{\mu} \tag{5.14}$$

Consider self-consistent method. Using (4.29), one may derived the following effective yielding potential,

$$\boxed{\Psi(\Sigma_{\rm eq}, \Sigma_{\rm m}, \mathbf{q}) = \frac{\Sigma_{\rm eq}^2}{\sigma_{\rm Y}^2} + \frac{4\omega(1-v^2)}{3\beta\pi(1-2v)} \frac{f}{\sqrt{1-\left(\frac{\Sigma_{\rm m}}{\sigma_0}\right)^2}} - 1 = 0} \tag{5.15}$$

where $\Sigma_{\rm eq}$ and $\Sigma_{\rm m}$ are defined as the macro-equivalent stress and mean stress, and $\mathbf{q}$ represents the other internal variables, which may be implicitly embedded in $\sigma_{\rm Y}$.

In terms of the ratio $\Sigma_{\rm m}/\sigma_{\rm Y}$, the effective yielding potential function of plastic flow Ψ can be finally recast as follows,

$$\boxed{\Psi(\Sigma_{\rm eq}, \Sigma_{\rm m}, \mathbf{q}) = \frac{\Sigma_{\rm eq}^2}{\sigma_{\rm Y}^2} + \frac{4\omega(1-v^2)f}{3\beta\pi(1-2v)} \left\{ \frac{1+\left[\left(\frac{4\sigma_{\rm Y}}{(1-2v)\Sigma_{\rm m}}\right)^2 - 3\right]^{1/2}}{\left[\left(1+\left[\left(\frac{4\sigma_{\rm Y}}{(1-2v)\Sigma_{\rm m}}\right)^2 - 3\right]^{1/2}\right)^2 - 16\right]^{1/2}} \right\} - 1 = 0} \tag{5.16}$$

The damage evolution equation may be derived in a similar fashion as the derivation of Gurson model (e.g. [14,40]).

6. Concluding remarks

The most distinguishing features of the present cohesive crack damage model are:

1. The homogenized macro-constitutive relations are different from the micro-constitutive relations: the reversible part of macro-constitutive relation is nonlinear elastic versus the linear elastic behaviors at micro-level; the irreversible part of macro-constitutive relation is a form of pressure sensitive plasticity versus the Huber–von Mises plasticity or cohesive laws at micro-level.
2. When the ratio of macro-hydrostatic stress and the true yield stress reaches a finite value, i.e.

$$\frac{\Sigma_{\rm m}}{\sigma_0} \to 1 \Rightarrow \frac{\Sigma_{\rm m}}{\sigma_{\rm Y}} \to \frac{4}{\sqrt{12}(1-2v)} \tag{6.1}$$

the cohesive damage model will predict a complete failure of material even if the amount of damage is infinitesimal. This fact is characterized by the vertical asymptote in Fig. 7(c). whereas in the [13,14], when the amount of damage is infinitesimal the material will not completely fail unless the hydrostatic stress becomes infinite. This fact is characterized by the horizontal asymptote in Fig. 7(d). Obviously, the Gurson model is not realistic, because it fails to predict material failure at its theoretical strength. In reality, no material can sustain infinite hydrostatic stress, and any material will fail if hydrostatic stress reaches to its theoretical strength, no matter there is crack or not. The newly proposed cohesive damage model is capable to predict this physical phenomenon.

3. In the cohesive damage model, the effective yield surfaces as well as damage evolution equations depend on materials Poisson's ratio; whereas in the Gurson model, no such dependence can be predicted, because of the assumption of incompressible RVE.
4. The rate of damage accumulation may depend on the rate of elastic deformation.

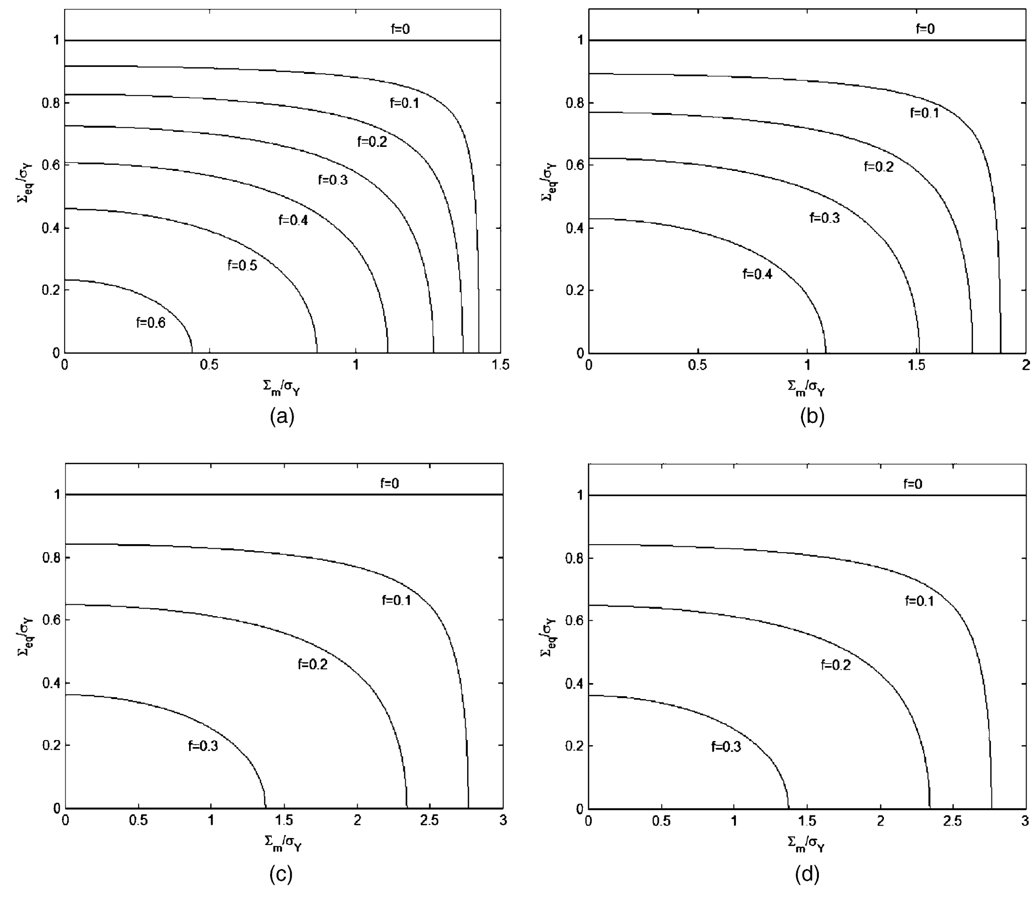

Fig. 6. Cohesive micro-crack damage model, $\Psi(\Sigma_{eq}, \Sigma_m, \mathbf{q})$, with different Poisson's ratios ($\beta = 1/3$): (a) $\nu = 0.10$; (b) $\nu = 0.2$; (c) $\nu = 0.25$; (d) $\nu = 0.3$.

The damage model, i.e. the newly derived pressure-sensitive yielding function Ψ, is displayed in Fig. 6 with different Poisson's ratios. In Fig. 7, the cohesive damage model is juxtaposed with the Gurson model for comparison.

It should be mentioned that the self-consistent scheme based damage model Ψ will fails at $\nu = 0.5$, since for incompressible elastic materials, uniform triaxial tension load will not be able to produce dilatational strain energy.

The key step in the energy method is how to accurately determine the energy release contribution to the material damage process. The energy release in nonlinear fracture mechanical process is consumed in several different dissipation processes, e.g. surface separation, dislocation movement and hence plastic dissipation, heat conduction, and may be even phase transformation, etc. Usually, the energy release contribution to damage process is only referred to the surface sepa-

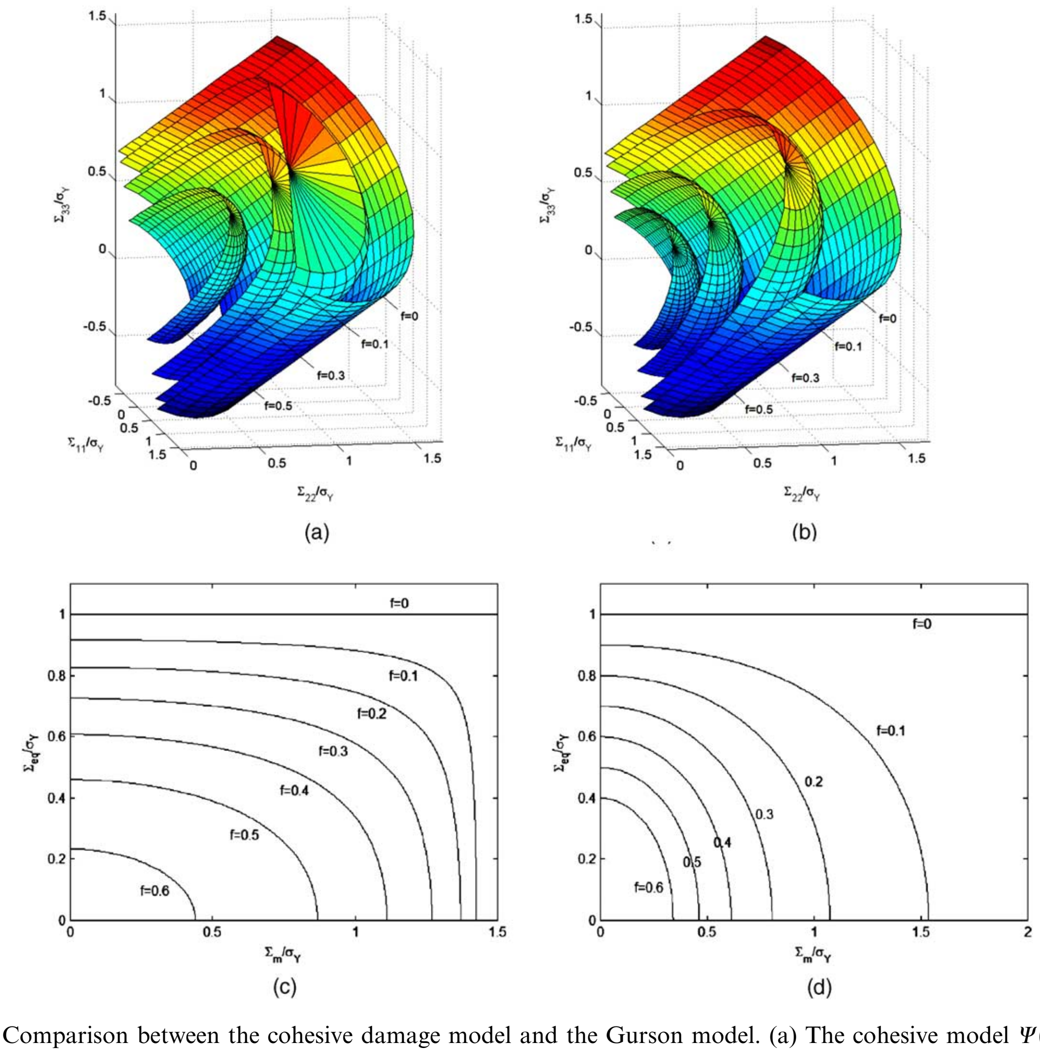

Fig. 7. Comparison between the cohesive damage model and the Gurson model. (a) The cohesive model $\Psi(\nu = 0.1)$; (b) the Gurson model; (c) the cohesive model $\Psi(\nu = 0.1)$; (d) the Gurson model.

ration energy release. In fact, both [28,42] have studied energy release caused by the extension of Dugdale-BCS cracks in a two-dimensional space. To incorporate those available results into the current formulation, an in-depth study may be needed to refine the damage model proposed here.

It is speculated that by considering interaction induced coalescence among cohesive cracks, one may be able to find a critical micro-crack opening volume, f_c based on analytical solutions, e.g. Dugdale-BCS cracks, the solution of periodically distributed cohesive crack [3].

Finally, one may notice that Eq. (3.42) provides a relationship between physical cohesive strength, σ_0, and the true (micro) yield stress, σ_Y,

$$\frac{\Sigma_m}{\sigma_0} = \frac{4}{1 + \sqrt{\left(\frac{4}{1-2\nu}\frac{\sigma_Y}{\Sigma_m}\right)^2 - 3}} \tag{6.2}$$

It gave an impression that the relationship between the two parameters depends on the macro-hydrostatic stress state, Σ_m.

To gain the insight of this relationship, Eq. (6.2) is plotted with different Poisson's ratio in Fig. 8. One may find that when $0 < \Sigma_m/\sigma_0 < 1$, the cohesive stress is almost proportional to the initial yield stress (see curves O–A_i, $i = 1, 2, 3$ in Fig. 8). This linear relationship can be approximated as

$$\sigma_0 \approx \frac{4}{\sqrt{12}(1-2\nu)}\sigma_Y \tag{6.3}$$

Therefore for all practical purposes, the assumption of a constant cohesive stress inside cohesive zone is consistent with the concept of constant yield stress.

Finally, it should be commented that the proposed damage model is only valid under the assumption that the density of the cohesive micro-crack distribution is small. As the density of

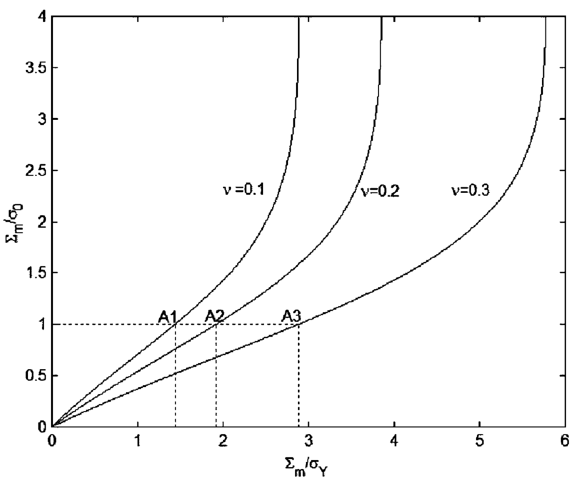

Fig. 8. Relationship between physical cohesion and true yield stress.

micro-crack distribution increases, it may lead to micro-crack coalescence or a drastic growth of an individual crack. Then the damaged material may become anisotropic in a local region, and it may soon lead to catastrophic failure. Therefore, the cohesive damage model proposed in this paper may not be able to describe the overall constitutive behaviors of the damaged materials at the later stage (see: [22]).

Acknowledgements

The authors would like to acknowledge Mr. Wei-Kam Li's early participation in this research project. The support (BURNL-07427-11503-EGSLI) by the committee on research of University of California at Berkeley is appreciated.

References

[1] G.I. Barenblatt, The formation of equilibrium cracks during brittle fracture, Journal of Applied Mathematics and Mechanics, [English translation PMM, vol. 23, 434] 23 (1959) 622.
[2] G.I. Barenblatt, Mathematical theory of equilibrium cracks in brittle fracture, Advances in Applied Mechanics 7 (1962) 55–129, Academic Press.
[3] B.A. Bilby, A.H. Cottrell, E. Smith, Plastic yielding from sharp notches, Proceedings of Royal Society of London, Series A 279 (1964) 1–9.
[4] B. Budiansky, J.R. Rice, Conservation laws and energy release rates, ASME Journal of Applied Mechanics 26 (1973) 201–203.
[5] B. Budiansky, R.J. O'Connell, Elastic moduli of a cracked solid, International Journal of Solids and Structures 12 (1976) 81–97.
[6] W.R. Chen, L.M. Keer, Fatigue crack growth in mixed mode loading, ASME Journal of Engineering Materials and Technology 113 (1991) 222–227.
[7] W.R. Chen, L.M. Keer, Mixed-mode fatigue crack propagation of penny-shaped cracks, ASME Journal of Engineering Materials and Technology 115 (1993) 365–372.
[8] D.S. Dugdale, Yielding of steel sheets containing slits, Journal of Mechanics and Physics of Solids 8 (1960) 100–104.
[9] J.D. Duva, J.W. Hutchinson, Constitutive potentials for dilutely voided nonlinear materials, Mechanics of Materials 3 (1984) 41–54.
[10] N. Fleck, Brittle fracture due to an array of microcracks, Proceedings of the Royal Society (London) A432 (1991) 55–76.
[11] M. Gologanu, J.B. Leblond, J. Devaux, Recent extensions of Gurson's model for porous ductile metals, in: P. Suquet (Ed.), Continuum Micromechanics, Springer-Verlag, 1995, pp. 61–130.
[12] A.E. Green, W. Zerna, Theoretical Elasticity, second ed., Oxford University Press, 1968.
[13] A.L. Gurson, Plastic flow and fracture behavior of ductile materials incorporating void nucleation, growth and interaction, Ph.D. Thesis, Brown University, Rhode Island, 1975.
[14] A.L. Gurson, Continuum theory of ductile rupture by void nucleation and growth: Part I. Yield criteria and flow rules for porous ductile materials, ASME Journal of Engineering Materials and Technology 99 (1977) 2–15.
[15] von H. Hencky, Zur theorie plastischer deformationen und der hierdurch im material hervorgerufen nachspannungen, rnal = Zeits. ang. Math. Mech. 4 (1924) 323–334.
[16] R. Hill, Elastic properties of reinforced solids: some theoretical principles, Journal of the Mechanics and Physics of Solids 11 (1963) 357–372.
[17] R. Hill, Theory of mechanical properties of fiber-strengthened materials-III: Self-consistent model, Journal of the Mechanics and Physics of Solids 13 (1965) 189–198.

[18] R. Hill, A self-consistent mechanics of composite materials, Journal of the Mechanics and Physics of Solids 13 (1965) 213–222.
[19] M. Kachanov, Effective elastic properties of cracked solids: critical review of some basic concepts, Applied Mechanics Review 45 (1992) 304–335.
[20] M. Kachanov, Elastic solids with many cracks and related problems, in: J.W. Hutchinson, T.Y. Wu (Eds.), Advances in Applied Mechanics, vol. 32, Academic Press, New York, 1994, pp. 259–445.
[21] L.M. Keer, T. Mura, Stationary crack and continuous distributions of dislocations, Proceedings of The First International Conference on Fracture, The Japanese Society for Strength and Fracture of Materials 1 (1965) 99–115.
[22] M. Hori, S. Nemat-Nasser, Interacting micro-cracks near the tip in the process zone of a macro-crack, Journal of Mechanics and Physics of Solids 35 (1987) 601–629.
[23] J.W. Hutchinson, Crack tip shielding by micro-cracking in brittle solids, Acta Metallurgica 35 (1987) 1605–1619.
[24] J.W. Ju, K.H. Tseng, Effective elastoplastic behavior of two-phase ductile matrix composites: a micromechanical framework, International Journal of Solids and Structures 33 (1996) 4267–4291.
[25] J.W. Ju, L.Z. Sun, Effective elastoplastic behavior of metal matrix composites containing randomly located aligned spheroidal inhomogeneities. Part I: Micromechanics-based formulation, International Journal of Solids and Structures 38 (2001) 183–201.
[26] L.Z. Sun, J.W. Ju, Effective elastoplastic behavior of metal matrix composites containing randomly located aligned spheroidal inhomogeneities. Part II: Applications, International Journal of Solids and Structures 38 (2001) 203–225.
[27] M.K. Kassir, G.C. Sih, in: Mechanics of Fracture: Three-dimensional Crack Problems, vol. 2, Noordhoff International Publishing, Leyden, 1975.
[28] A.P. Kfouri, Crack separation energy-rates for the DBCS model under biaxial modes of loading, Journal of Mechanicsand Physics of Solids 27 (1979) 135–150.
[29] D. Krajcinovic, Damage mechanics, Elsevier, Amsterdam, New York, 1996.
[30] V. Lubarda, D. Krajcinovic, Damage tensors and crack density distribution, International Journal of Solids and Structures 30 (1993) 2859–2877.
[31] V. Lubarda, D. Krajcinovic, Tensorial representation of the effective elastic properties of the damages material, International Journal of Damage Mechanics 3 (1994) 38–56.
[32] F.A. McClintock, A criterion for ductile fracture by the growth of holes, ASME Journal of Applied Mechanics 35 (1968) 363–371.
[33] T. Mura, Micromechanics of Defects in Solids, Martinus Nijhoff Publishers, Dordrecht, 1987.
[34] S. Nemat-Nasser, M. Hori, Micromechanics: overall properties of heterogeneous materials, second ed., Elsevier, Amsterdam–Lausanne–New York–Oxford, 1999.
[35] T. Pardoen, J.W. Hutchinson, An extended model for void growth and coalescence, Journal of the Mechanics and Physics of Solids 48 (2000) 2467–2512.
[36] J.R. Rice, A path independent integral and the approximate analysis of strain concentration by notches and cracks, ASME Journal of Applied Mechanics 35 (1968) 379–386.
[37] J.R. Rice, Mathematical analysis in the mechanics of fracture, in: H. Liebowitz (Ed.), Fracture: An Advanced Treatise, vol. 2, Academic Press, 1968, pp. 191–311.
[38] V. Tvergaard, Influence of voids on shear band instabilities under plane strain conditions, International Journal of Fracture 17 (1981) 389–407.
[39] V. Tvergaard, On localization in ductile materials containing voids, International Journal of Fracture 18 (1982) 237–251.
[40] V. Tvergaard, A. Needleman, Analysis of the cup-cone fracture in a round tensile bar, Acta Metallurgica 32 (1984) 157–169.
[41] V. Tvergaard, Material failure by void growth to coalescence, in: J.W. Hutchinson, T.Y. Wu (Eds.), Advances in Applied Mechanics, vol. 27, Academic Press, New York, 1990, pp. 83–151.
[42] M.P. Wnuk, Mathematical modeling of nonlinear phenomena in fracture mechanics, in: M.P. Enuk (Ed.), Nonlinear Fracture Mechanics, Springer-Verlag, Wien-New York, 1990, pp. 359–451.